VĚDECKÉ SPISY VYSOKÉHO UČENÍ TECHNICKÉHO V BRNĚ

Edice PhD Thesis, sv. 625

ISSN 1213-4198

Ing. Jan Boháček

Effect of Flow Parameters of Water and Air Atomized Sprays on Cooling Intensity of Hot Surfaces

BRNO UNIVERSITY OF TECHNOLOGY
Faculty of Mechanical Engineering
Heat Transfer and Fluid Flow Laboratory

Ing. Jan Boháček

EFFECT OF FLOW PARAMETERS OF WATER AND AIR ATOMIZED SPRAYS ON COOLING INTENSITY OF HOT SURFACES

Vliv ostřikových parametrů vodních a vodovzdušných trysek na intenzitu ochlazování horkých povrchů

SHORT VERSION OF PHD THESIS

Branch:	Engineering Mechanics
Supervisor:	doc. Ing. Jaroslav Horský, CSc.
Opponents:	doc. Ing. Pavel Rudolf, Ph.D. Ing. Pavel Střasák, Ph.D.
Date of defence:	14. 4. 2011

Key Words:

Droplet, vapor layer, film boiling, jet atomization, solid jet, flat jet, cooling nozzles, user defined function, UDF, Volume of Fluid model, Lagrange particles, surface tension model, interface normal, curvature, Continuum Surface Force, HTC, Fluent, CFD

Klíčová slova:

kapka, parní vrstva, blánový var, atomizace sprejů, válcový paprsek, plochý paprsek, chladicí tryska, uživatelsky definovaná funkce, Lagrangeovy částice, povrchové napětí, normála k volné hladině, křivost, CSF, Fluent, výpočtové modelování proudění

PhD thesis deposited in:

Areálová knihovna FSI VUT v Brně (Technická 2896/2, 616 69, BRNO)

ISBN 978-80-214-4296-2
ISSN 1213-4198

Content

1 INTRODUCTION

By the word primary steel processing, we mostly understand continuous casting, centrifugal casting but also hot and cold rolling. Heat transfer is the most characteristic and prevailing process for all of them, which may be attended by other side processes such as solidification, mechanical deformation, oxidation, and so on. To ensure perfect quality of final products the cooling control is naturally desirable. It requires the cooling intensity to be optimized. In majority cases the needed cooling is provided by arrays of nozzles in that the operating fluid is the most frequently water but also mixture of both, air and water, and last but not least different emulsions supporting better lubrication of working surfaces. In particular, it is the cooling intensity that is responsible for the final quality of product, and thus the cooling system should be reasonably designed in terms of not only suitable cooling but also energy savings. Essentially, four different ways can be used to design a cooling system. Designers often rely on their own experiences and proceed intuitively. Another way is the using of some of plenty correlations that were put together based on experimental data and allow to calculate heat transfer coefficient as a function of flow parameters. However, those correlations are always restricted to a certain range of selected parameters, hardly ever account for more than one nozzle or even curved surfaces. The most sophisticated and precise method is seemingly a laboratory experiment and the consequent inverse task, which is capable of the thermal boundary condition reconstruction. Performing of experiments is however economically and energy demanding and that's why it gives a chance to Computational Fluid Dynamics that are capable of simulating fields of velocities, pressures, temperatures numerically provided boundary conditions are correctly defined and appropriate models are employed. It is CFD that is the background of this thesis and hopefully brings new pieces of knowledge into cooling problems solved numerically with the help of CFD methods.

1.1 OBJECTIVES OF THESIS

The main objective is to deal with the description of several cooling processes numerically namely using the commercial CFD software Fluent. Here, it could be further assigned to two categories. The first category should cover the microscopic point of view i.e. a single droplet approaching, hitting and spreading on a hot surface. The second category should comprise heat transfer simulations of an entire jet emanating from a particular nozzle. The solid jet and the flat fan nozzles were chosen as representatives to be simulated. Type of the solid jet nozzle was chosen from experimental paper work of other researchers in order to allow for verification

of calculated data. However, the selected flat fan nozzle can be found in the real continuous slab caster as a basic cooling unit in the secondary cooling system.

Imagine a hot steel plate of the thickness in order of millimeters or centimeters with one side exposed to a spraying jet that involves a very intensive cooling. Thermal boundary condition in the jet footprint and surroundings is naturally unknown, time dependent and changes along with surface temperature, flow parameters and physical properties of the operating fluid. On the other hand, other thermal boundary conditions around are either usually known or can be easily defined considering some simplifying assumptions e.g. an adiabatic wall etc.

The computational domain must be extended to fluid region i.e. the region where the jet is spraying, so that the heat transfer can be solved using CFD methods. The extension must be sufficient enough in order to define accurate boundary conditions.

In solid region it is only the equation of unsteady heat conduction to be solved whereas in fluid region it is Navier-Stokes equation modified for two phase flow that has to be primarily solved along with continuity equation. Further, there are energy equation and equations for turbulent properties in fluid region. Fluid region, which is described by several partial differential equations, is obviously more complicated in terms of numerical schemes than solid region described only by a single diffusion equation. According to underlying physics and flow nature the most suitable multiphase model can be selected that is however still rather general and has to be concretized via extra subroutines.

1.2 DESCRIPTION OF MULTIPHASE MODELS

Three absolutely different multiphase models were used to describe physics of the foregoing objectives. Basic principles of these models are briefly summarized below.

The Volume of Fluid method (VOF) is the first multiphase model, which belongs to so-called interface tracking methods (e.g. the front-tracking method, the Level-Set method, the boundary integral method, the Second Gradient method etc.) and is able to capture the actual position of interface. In other words, it does not enable to simulate the flow of dispersed phase. The color function F stands for the basic idea of the VOF model and represents the fractional volume of the cell. F = 1 means that the cell is occupied by the fluid, while a zero value indicates that the cell contains no fluid. Cells with F values between zero and one must then contain free boundary. The function F can be expressed as the following

$$F = \frac{V_{sp}}{V_{cell}}$$

where V_{sp} is the volume of the secondary phase within the cell with the volume of V_{cell}. The scalar function F is tracked either implicitly i.e. additional transport equation is solved or is evaluated explicitly. Besides, the continuity and the momentum equations must be solved simultaneously. Both terms on left side of the continuity equation contains the function F in the numerator. The VOF model is well-known and widely used since it is mass conservative and robust, but it also suffers from several bottlenecks. For transverse flows or triangular meshes it may suffer from interface smearing. It requires nearly one order lower computational time step to satisfy stability condition. The basic stability condition originally proposed by Brackbill has the following form

$$\Delta t_\rho \sim \sqrt{c_1 \frac{\rho}{\sigma} \Delta x^3}$$

It should be noted that in literature (Vigneaux) different stability condition can be found for low Reynolds flows; hence, using the Brackbill's stability condition is ambiguous. For many interfacial flows Capillary forces cannot be neglected. Whether surface tension effects are important or not can be judged by Capillary and Weber numbers. In the VOF model surface tension is modeled via the Continuous Surface Force model (CSF), which as shown later can fail or even cripple the main flow. Surface tension force is naturally applied as a volume source and interface normals and curvatures are calculated from the gradient of rather stepwise color function F.

Considering the description of the first multiphase model, the VOF model, as completed, several words can be mentioned on the second multiphase model. Unlike the VOF model, the Euler-Euler model handles two or more phases as miscible fluids with one phase denoted as a primary phase and the rest denoted as dispersed phases. The momentum and the mass balance are calculated for each phase separately. When the flow is turbulent, it is also possible to solve turbulence separately for each phase. The interphase momentum exchange is provided via volume source terms for accompanying forces such as the drag force, the lift force etc.

As regards the third multiphase model, the Discrete Phase model (DPM), the continuous phase flow is solved by the time-averaged Navier-Stokes equations, while the dispersed phase is treated as a large number of particles, droplets that are tracked through the whole computational domain and can exchange momentum, mass and energy with the continuous phase. The basic form of continuity and momentum equation for the continuous phase remains the same except of one term. It is the term corresponding to momentum exchange between the continuous and the

dispersed phase. The trajectory of droplets is calculated by integration of the force balance on each particle mass in a Lagrangian frame of reference. In Cartesian coordinates this force balance is written as

$$\frac{du_{di}}{dt} = F_D\left(u_i - u_{Di}\right) + \frac{g_i}{\rho_p}\left(\rho_p - \rho\right)$$

where F_D is the drag force and the second term on the right side accounts for the gravity force and the buoyancy force. The flow of the continuous flow influences the flow of the dispersed phase and vice versa i.e. it is coupled. Regarding the heat transfer, in the case of the continuous phase the transport equation for enthalpy is solved. On the contrary, the temperature of each particle is constant throughout and is given by a simple ordinary differential equation

$$m_d c_{dp} \frac{dT_D}{dt} = hA_d\left(T_\infty - T_d\right)$$

where the right hand side determines the actual physics of particle heating. For example, this equation denotes a convective heating. Besides, other heating laws for different heating mechanisms such vaporization, boiling can be considered.

2 SINGLE DROPLET SIMULATIONS

Originally, the plan was to simulate a single droplet impinging onto a hot surface, the consequent spreading of the droplet, and most importantly the distribution of heat transfer coefficient (HTC) dependent on radial position and time. Note that the most of nozzles for cooling purposes produce very fine droplets (SMD~100 μm). Therefore, droplets of this size were of interest. However, for such a small droplet problems related to modeling of Capillary forces were detected and thus, the original schedule was partially modified to the flow study of free-falling droplet and the closely related surface tension modeling.

2.1 THEORY

Momentum is generally transferred between both, air and water phases, through mass transfer interphase drag, lift, gravity and buoyancy. The lift force is important when the density of droplet is much lower than density of ambient, e.g. bubbly flows. Hence, the lift force can be neglected. Further, buoyancy force can be also neglected due to very low density of air. Then the force balance on the droplet can be written as:

$$m\frac{dv}{dt} = mg - C_D A \rho_g \frac{v^2}{2}$$

where C_D is the drag coefficient. In general, the drag coefficient C_D is a function of particle shape and its orientation with respect to the flow, Reynolds number, turbulence level and Mach number.

Here, a new drag law was suggested based on experimental data and is valid up to Re=1000. The correlation is as follows:

$$C_D = \mathrm{Re}^{-0.9116} \cdot \exp(0.04833 \cdot \log(\mathrm{Re})^2 + 3.2983)$$

The equation for the force balance was solved using the Runge–Kutta method in Matlab and calculated acceleration and corresponding velocities were used to verify simulations. Two droplet diameters were considered (2 mm, 0.2 mm). Besides velocity behavior, terminal velocities (6.37 m/s, 1.8 m/s) were calculated respectively.

2.2 TERMINAL VELOCITY OF DROPLET, CFD

Here, simulations were supposed to prove whether the VOF model along with the CSF model is able to calculate terminal velocity of droplet. This task was solved in the droplet frame of reference, which in simple terms means that the droplet was motionless and air flowed around the droplet. The velocity of far field was then the terminal velocity of droplet. The advantage of this model is that there is no need for the dynamic mesh refinement since the droplet remains at the same position. Moreover, mesh can be precisely refined in regions of steep velocity or pressure gradient. The terminal velocity of 6.56 m/s was calculated for 2mm droplet that agrees quite well with the ODE solution. In the case of 0.2mm droplet, the terminal velocity did not converge to a single value, but rather oscillated between 1.8–2.0 m/s. As shown later the CSF model was the responsible factor. Mesh, contours of velocity and path lines for the 2mm droplet are illustratively shown in Fig.1. Due to the shear stresses in the vicinity of the interface, the water circulated with the maximal axial velocity magnitude of 0.2 m/s and the wake of the length nearly of 5 mm is formed behind the droplet.

2.3 VELOCITY FIELD INSIDE AND OUTSIDE DROPLET, CFD

A short excursion was made to seek for an easier and faster way of simulating velocity and pressure field outside and inside the droplet. The speedup consisted in using only single phase model and steady solver. Considering the spherical droplet, the interface was represented by a rigid wall and the momentum exchange through the interface was provided via user defined functions. Simulations were more than

20 times faster than the aforementioned VOF calculations and results were in good agreement.

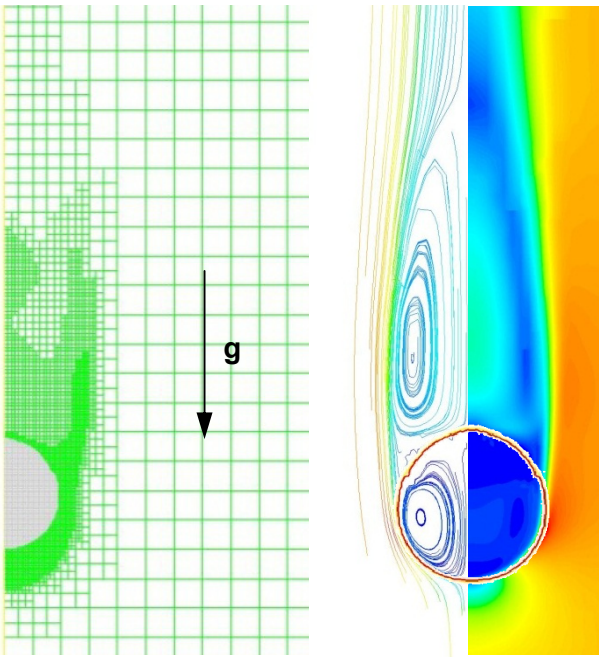

Fig.1 Mesh and velocity field around 2mm droplet at terminal velocity

2.4 DROPLET ACCELERATING IN GRAVITY FIELD

Here, a special procedure for dynamic mesh refinement along the droplet interface was developed and the effect of surface tension on the droplet acceleration was numerically studied. The initial velocity of droplet was zero; thus, the capillary forces and the gravity force were the only forces acting on droplet. Both droplets were simulated (2.0, 0.2 mm). Since only a very short time interval was simulated (0.05 s), the actual acceleration was constant i.e. there was a linear growth in droplet speed. The case with 2mm droplet fitted quite well the reality; however, the finer the mesh was the smaller the acceleration was. In the case of the 0.2mm droplet, the droplet even did not start falling but rather kept on vertical fluctuating around the position. When the surface tension was lowered enough, the droplet started falling, but only when the surface tension was turned on, the results followed the reality. In here, some bottlenecks of the surface tension model (CSF) were detected and studied later.

2.5 STUDY ON SPURIOUS CURRENTS

The purpose of this study was to observe the behavior of a 2mm droplet patched in the center of square domain assuming the Capillary force to be the only force acting on the droplet. Simulations with four different mesh densities were performed. For each case two different stability conditions were respected. The first

one was the original Brackbill's stability condition. The second more restrictive one was originally published by Vigneaux, who suggested it for low Re flows. Results were evaluated in terms of mean and maximum velocities detected within domain at dimensionless time τ. The choice of lower time step defined according to Vigneaux had negligible effect on spurious currents generated within domain. However, the mesh size significantly affected the flow. The finer the mesh was, the higher the velocities were calculated. Maximum velocities were about 0.2 m/s, whereas mean velocities were about 0.05 m/s excluding air cells from calculation. The fundamental findings can be summarized into one sentence. For fine grids the CSF model diverges with mesh refinement. As a next step procedures for calculation of normals and curvatures were inspected.

2.6 INTERFACE NORMAL, CURVATURES AND SURFACE TENSION AS SOURCE TERM

Four different approaches were employed to calculate interface normals. First two approaches simply calculated normals from gradient macro C_VOF_G(c,t) and reconstructed gradient macro C_VOF_RG(c,t) available through UDFs. The third approach was the ALE-like scheme, which is most likely the same as the second macro mentioned above. Unlike the macros, the using of this approach required a knotty user defined functions, since accessing of for neighboring cells was necessary. Even more complicated functions had to be used in the last approach employing so-called Height Functions. Height Functions were constructed within each cell containing interface with help of either horizontal (3x7 cells) or vertical (7x3 cells) stencil. The accuracy of those four procedures was assessed with the help of maximum and mean deviation of calculated normal from the actual normal. The most accurate results were gained by using the HF approach. The maximum deviation was 0.76°, while the mean deviation was only 0.26°. On the contrary, the worst results were obtained with the gradient macro C_VOF_G(c,t). The maximum deviation was 5.0°, while the mean deviation was only 1.74°. HFs can obviously capture normals to interface more precisely than standard procedure simply based on gradient of the color functions F. Besides interface normals, it was also important to calculate curvatures. It was done only for normals calculated using ALE-like scheme and HF approach. In most of interface cells, ALE-like scheme gave satisfactory results within error of 1 %; however, in some cells errors were even higher than 100 %. The HF approach again showed better capabilities. In most normal directions to the mapped mesh errors were insignificant, but in transverse direction it was still nearly 40 %.

In here, a new method for curvature calculation was imposed. Knowing normal previously calculated using HFs, the interface can be reconstructed using piecewise linear elements. In 2D, each linear element has two intersection with corresponding cell faces. These intersections within the current interface cell and also intersections within two neighboring cells are used to construct three circles from three points. Circle centers are then identified, averaged into one value, and new curvature corresponds to reciprocal value of distance from the circle center to the current interface cell.

In FVM based methods the surface tension must be applied as a volume source term even though it acts as a surface force. In the CSF approach the source term is rather non-zero even outside the interface because it comprises the color function F. The advantage is that the volumetric force is now evenly distributed along interface no matter the grid orientation; the exact position of interface is not needed. The disadvantage is that there is not the prompt jump in pressure across the interface and as issued here, parasitic currents occur especially in cases with high density or viscosity ratios. Therefore, a new model was suggested which comprised the reconstructed length of interface. The main idea consisted in imposing the surface tension at a virtual interface that was created by shifting the actual interface either into the denser phase or into the more viscous phase depending on whether the density or the viscosity ratio is more important. The shift was as small as possible, but big enough to ensure the position of virtual interface entirely in cells containing only one phase.

3 SIMULATIONS OF JETS, ATOMIZED JETS

Generally, when the jet emanating from an arbitrary nozzle either does not undergo a breakup into fine droplets or it breaks into large liquid bunches at the most, then one of free surface tracking methods should be certainly used. On the other hand, when the ultimate breakup is expected e.g. for high Weber numbers, then it is commonly mandatory to employ multiphase models for miscible phases such as the Euler-Euler or the Euler-Lagrange model.

3.1 SOLID JET

The solid jet of 2 mm diameter impinging onto hot cylindrical surface (diameter of 6 mm) was simulated for flow rate of 1.2 l/min. The corresponding outlet velocity was 6.4 m/s. The nozzle-to-wall distance was 10.6 mm.

The k-epsilon model was used to capture turbulence, although the RNG model is generally not recommended for flows with significant streamline curvatures, swirl

and rapid changes. It was preceded by the tuning of turbulent Prandtl number Pr_t, which directly influences the effective thermal conductivity. This model constant Pr_t was set based on simulations of flow around a horizontal plate and credible correlations for Nusselt number. The default value of 0.85 had to be replaced by 1.3 in order to fit correlated data.

Concerning the solid jet, first simulations were performed for thermal boundary condition that led only to the conductive and the conductive heat transfer i.e. no phase changes could occur. The constant heat flux of 398 kW/m2 was set on the impact wall. When a jet impinges a wall, the flow near the jet axis undergoes relaminarization and in a certain distance the transition back to turbulence takes place again. In this case, the exact position of the transition was found based on literature survey. The following model thus accounted for the transition from the laminar to the turbulent flow. In Fig.2 nearly the entire computational domain is shown, where contours of velocity are shown along with distribution of heat transfer coefficient. Red dots stand for experimental data, whereas orange and yellow curve represent results from simulations. Results are in a very good agreement.

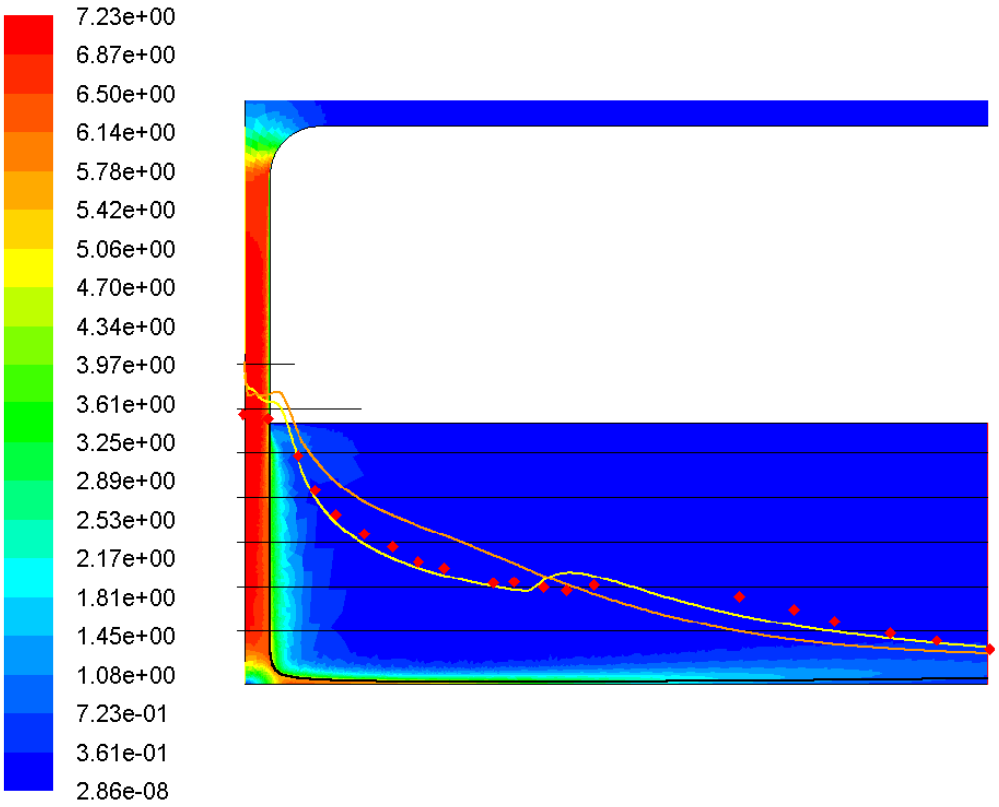

Fig.2 Spreading of unconfined water jet on hot wall with illustrative trend of HTC; contours of velocity magnitude [m/s]; red points (Wu's experiment), orange curve (calculation with k-epsilon model), yellow curve (accounts for transition to turbulence)

In the next step a new model was suggested to account for the film boiling. The vapor layer was expected to be continuous with time independent thickness. The first occurrence of the vapor layer was expected when the liquid reached the temperature of 150 °C as claimed in literature. This model was drafted for the steady state solver; therefore, the main assumptions are: the thickness of vapor layer is time independent and only film boiling can occur i.e. condensation cannot be modeled. The UDF was designed to calculate vapor mass and energy sources for continuity and energy equation. The algorithm was designed as follows. Firstly, the closest cell to the jet axis near impact wall with temperature of 150 °C was detected. Since the vapor layer formation was expected to start inside this cell, the vapor mass source term was imposed. Secondly, vapor flow rate through the outlet boundary condition was checked every each iteration. As soon as it was the same as the sum of vapor mass sources, new source terms were imposed in downstream cell and the algorithm looped until interface had the saturation temperature. The procedure is schematically shown in Fig.3.

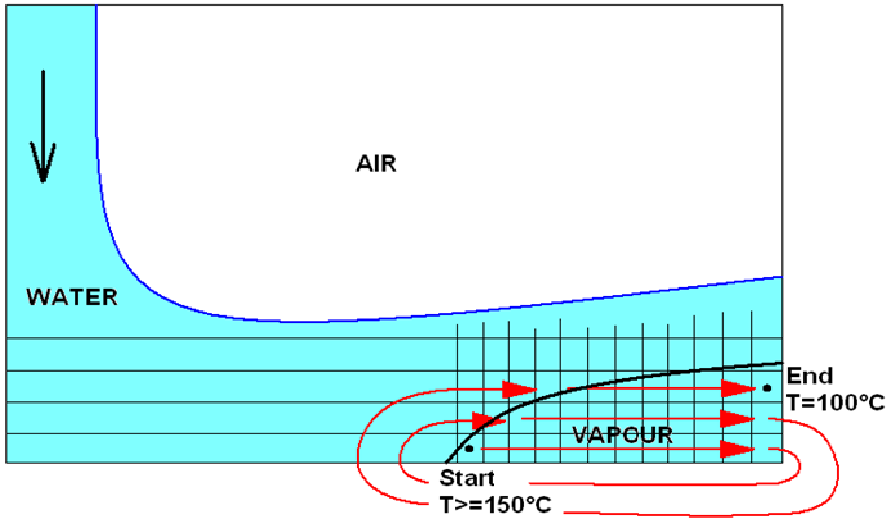

Fig.3 Illustrative outline of looping algorithm for deriving source terms

Besides, another model for film boiling was developed based upon work by Welch and Yuan. Unlike the aforementioned approach, here, the vapor layer can be continuous, but it can also oscillate and even break into small bubbles. Both, evaporation and condensation could be simulated. Source terms were either imposed in cells containing interface or in cells adjacent to the hot wall. Within each of these cells the heat flux was calculated using the following expression:

$$Q = k\frac{dT}{dn_i} = k\left(\frac{dT}{dx_i}\cdot n_i\right)/|n_i| \quad [W/m^2]$$

Knowing the heat flux, the basic mass source term is given by the next formula:

$$S_{vapor} = \frac{A \cdot Q}{L \cdot V}$$

where A is the area of interface demarcated by cell faces. The latent heat is denoted by L. Finally, the cell volume is labeled as V. Other related source terms come out from this source.

In addition to the VOF simulations, the Euler-Lagrange model was used instead. First, the only the cold flow was studied in terms of velocity profiles in different positions. The distribution of impact pressure was compared with previous VOF simulations. At last, several heat transfer simulations were performed considering firstly only the inert heating of droplets and then also the evaporation of droplets. Besides, the UDF was developed to customize the default inert heating law, which allowed for the control of heat transfer coefficient on the droplet surface.

3.2 FLAT-FAN NOZZLE

Unlike the continuous flow emerging from the solid jet nozzle, the flat fan nozzle is intentionally designed to produce chisel-like water jet pattern consisting of fine droplets. Therefore, from the engineering point of view the using of the VOF model is impractical because of high computational demands and a different model should be used instead. Here, the Euler-Euler and the Euler-Lagrange models were employed.

The nozzle of interest was the manufactured Lechler 600.429.16.33 commonly used in the section of secondary cooling within the continuous slab caster. More specifically, this nozzle is a basic unit in first row of nozzles under the mold and above the foot rolls. (See Fig.5 for idea about the complete geometry). Multiphase simulations were preceded with the simulation of the cold flow that provided them with inlet boundary conditions (velocity components, volume fraction of liquid, turbulent kinetic energy and dissipation rate).

Note that dispersed phase could be rather formed into continuous phase in the gap between the foot roll and the slab. Hence, the mixture Euler-Euler was used considering the constant droplet diameter. Simultaneously, the simple breakup model was developed based on the WAVE model. The basic equation for the change of diameter of the parent droplet was supposed to follow this equation:

$$\frac{da}{dt} = -\frac{a-r}{\tau}, \quad (r \le a)$$

where τ is the breakup time. The radius of the parent droplet is denoted by a, and r is the radius of the new formed droplet. In Fig.4 iso-values of water volume fraction

clearly define the silhouette of the jet. The colormap within the nozzle footprint stands for the impact pressure. Several bottlenecks should be emphasized: the jet was unrealistically flat; a lack of dispersed phase was detected in the center line, simulation was very slow (Δt = 5e-06 s).

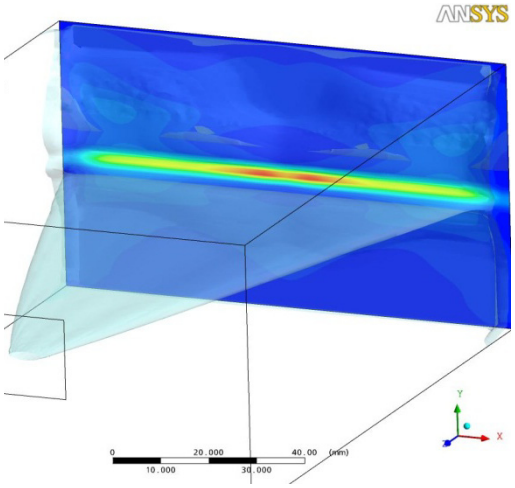

Fig.4 Iso-value of water volume fraction with contours of total pressure

Due to aforementioned bottlenecks, this modeling approach was left behind and the Euler-Lagrange model was considered instead. The primary breakup model was estimated using the standard Flat-fan atomizer model. Concerning the secondary breakup of droplets, two models were tested (the Taylor Analogy Breakup model and the Blob Jet model); however, only the TAB model gave reasonable results. See Fig.6 for information about distribution of droplet size. Both, experimental data and data from simulations are shown.

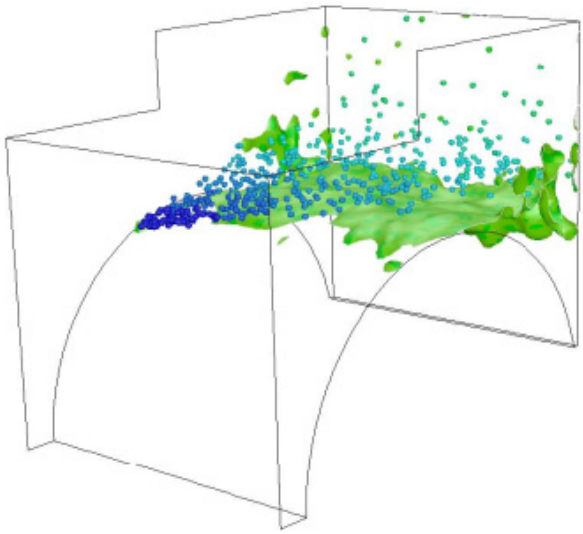

Fig.5 Isometric view of the whole computational domain with flat jet represented by water droplets and continuous water in gap between the slab and the foot roll (droplets are represented in blue, water volume fraction of 0.5 is in green)

Since droplets represented by Lagrange particles cannot cluster and thus form a continuous phase, the UDF was developed to couple the DPM and the VOF model. In other words, when the droplet hits the free water surface it exchanges momentum, and its mass is converted into the continuous phase. In Fig.5 the green surface represents the free water surface of the water bulk captured between the moving slab and the rotating foot roll.

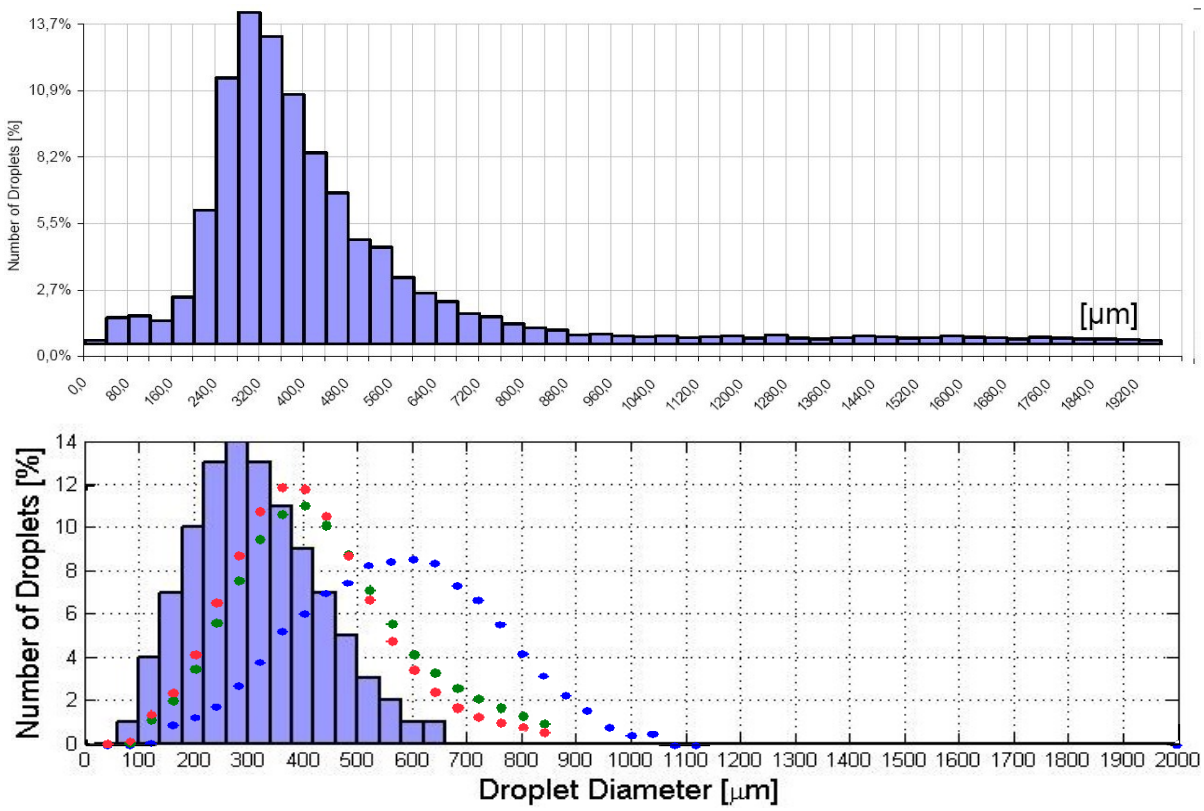

Fig.6 Droplet distribution from experiment (top), velocity distribution from simulations (bottom), red dotted line denotes the case with 10 streams and 1500 parcels, green dotted line denotes the case with 10 streams and 1000 parcels and blue dotted lined denotes the case with 10 streams and 50 parcels

So far, the cold flow was discussed. In the real casting process the temperature of the slab is fair above 1000 °C. For heat transfer simulations the temperature was lowered to 200 °C in order to avoid big source terms. The model settings were rather parametric with the following parameters sorted by effect: the mesh density, boundary condition for Lagrange particles, saturated vapor pressure, the number of streams. In Fig.7 the color map of heat flux within the nozzle footprint is shown.

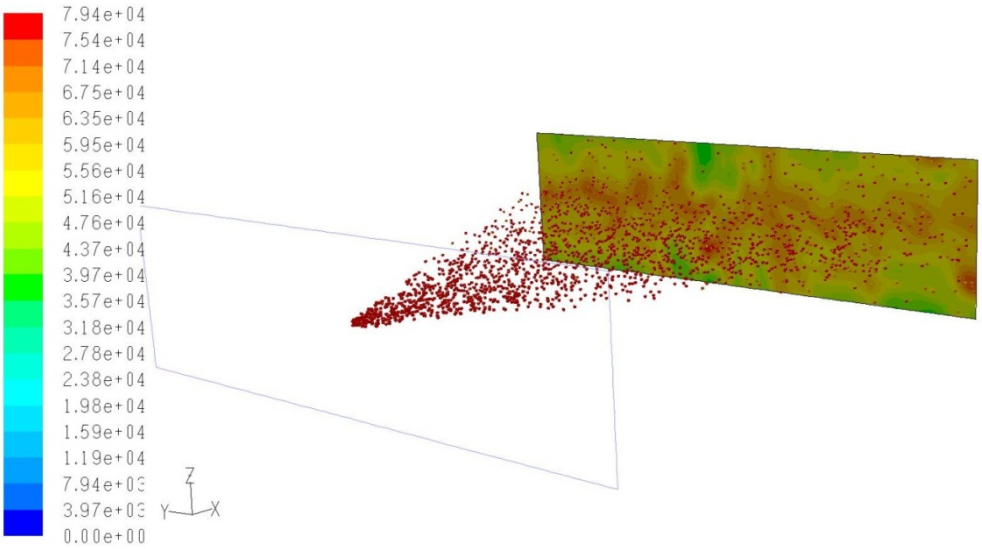

Fig.7 Droplets of flat jet and contours of heat flux [W/m^2]

4 DISCUSSION AND CONCLUSIONS

The title of thesis is Effect of flow parameters of water and air atomized sprays on cooling intensity of hot surfaces that obviously says nothing about procedures and approaches used to gain valuable results. Thus, the fact that solely CFD methods namely the commercial code Fluent were used is the first very important remark in conclusions. Furthermore, it is very important to note that unlike non-commercial in-house codes the CFD package Fluent as a general-purpose modeling tool does have a certain lack in flexibility and numerous lines must be inevitably respected. Anyway, even without additional user changes to Fluent's algorithms it is still capable CFD tool. As accidentally indicated it is possible to design your own user defined subroutines (UDFs) when a standard model suffers from incompleteness. UDFs in this thesis stand for a basic building stone.

The thesis is divided into two seemingly independent parts. The first part concerns numerical study of a single droplet denoted as a micro-scale point of view. The second part is dedicated to simulations of the entire water jet emanating from a solid jet nozzle and a flat fan nozzle using the Euler-Euler and the discrete phase model (DPM).

In the first part the detailed description of the free surface tracking model (Volume of Fluid, VOF) precedes results from simulations. In brief, the only difference compared to single phase flow modeling is that the volume fraction is used to track and identify the interface position. It was found out that in addition to the standard convective stability condition (CFL) a special stability condition exists

and must be obeyed. This stability condition prevents waves on free interface from being amplified. In single phase flow simulations the convective stability condition introduced by Courant number (CFL) should be less than 2. However, here in VOF simulations it was below 0.5.

The main objective of the first part was originally a comprehensive explanation of heat transfer coefficient (HTC) on a hot surface during a single water droplet impact and a consequent droplet spreading. Further, it was also intended to study the velocity field both outside and inside the moving droplet. First simulation settings were as the following. The droplet of the specified diameter was patched inside a two dimensional domain with the initial velocity of zero. In other words the droplet was static at the beginning of simulation. The gravity force, the capillary forces and the drag force were the only forces acting on the droplet. Naturally, the droplet velocity was expected to follow the Newton's law. Numerical solution of Newton's law (ODE solved in MATLAB) was used for verification of results from simulations. Note that the algorithm for Newton's law was also designed to account for the drag force considering both, constant and dynamic drag coefficients. Results from simulations unexpectedly varied significantly within the range of tested droplet diameters 2.0 - 0.2 mm. The case with 2mm droplet diameter agreed perfectly with Newton's law solved numerically. However, the case with the droplet diameter of 0.2 mm was far from to be desired because of so-called spurious or parasitic currents that appeared during simulation and prevented the droplet from the physical acceleration. For the smallest diameters the droplet even didn't start falling towards the bottom surface, it rather kept on fluctuating around the same position. These parasitic currents were evidently caused by the surface tension model (CSF - Continuum Surface Force model). Because of the presence of spurious currents especially in droplet diameters common during spray cooling the HTC distribution could not be for that reason studied. Instead of running meaningless simulations seeking for HTC distribution, several different models were set up in order to give detailed information on parasitic currents, droplet terminal velocities obtained from simulations, and proposals how to get rid of parasitic currents.

The first modeling approach was aimed at terminal velocity of free falling droplet. Simulations were carried out in the droplet frame of reference in order to maintain the droplet in the same position i.e. the droplet was without move and there was rather a non-zero velocity field around it. This approach allowed for static mesh refinement along the interface and in places of large velocity gradients. With help of this approach, pressure and velocity field could be studied with success, but unfortunately only in the case of 2.0mm droplet. This approach was also found to be

suitable for calculation of terminal velocity (2.0mm droplet ~ terminal velocity of 6.56 m/s). As regards the failure of the model in the case of 0.2 mm droplet, it was caused by some lacks of CSF model. Despite this weakness of the model, the terminal velocity (0.2mm droplet) agreed quite well with real droplet behavior (terminal velocity of 1.8 m/s). The model was able to capture the recirculation area inside the droplet and the wake formed behind it.

The purpose of the second modeling approach was to simplify the previous model in terms of forgetting multiphase models and using single phase model instead. The circular droplet was introduced as an axisymmetric circle surrounded by walls. The momentum transfer across the wall was provided through User Defined Function (UDF). This study gave satisfactory results as regards velocity and pressure field in full range of tested diameters. Note that it was not capable of computing terminal velocity. The terminal velocity was actually used as inlet velocity boundary condition. The advantage of this model was that simulations could be run within the steady solver and thus it greatly reduced computational time consequently. Just one remark on momentum transfer through the interface should be made: The UDF accessed velocities in fluid cells (air fluid) adjacent to the interface (wall) and then imposed a 'relevant' portion of stored velocities in each of counter-cells in droplet bulk. The 'relevant' portion of velocity is always less than unity and in this case, it was determined from the previous simulations.

The third model directly simulated a droplet free-fall under gravity with the help of the dynamic grid adaption procedure implemented via journal file. This model was used to study the effect of the CSF model on the droplet acceleration during the free fall. The droplet with the diameter of 2.0 mm was tested only on mesh sensitivity and it was found out that the finer the mesh was, the lower the resulting acceleration was. The actual droplet speed was nearly linearly dependent on time; however, in simulations the finer mesh led to the drop in droplet speed. That's why this model was also the confirmation of several paper works that the CSF model diverges with the mesh refinement. While the 2mm droplet was tested on mesh sensitivity, the 0.2mm droplet was tested within the range of different surface tensions. The physical value of surface tension (0.072 N/m) even completely prevented the droplet from falling. The droplet rather kept on fluctuating around the initial position. The lower the value of surface tension was, the more realistic the droplet acceleration was. This malfunction of the standard surface tension model (the CSF model) initiated the next step that was aimed at how normals, curvatures, and the entire CSF model are implemented into Fluent code. Before this was done, several simulations were performed without gravity in order to objectively study parasitic currents in terms of maximal and mean velocity values. Only the 2.0mm

droplet was considered and as expected, errors in velocities grew up with the mesh refinement. Maximal values of parasitic currents for the finest mesh (0.025 mm) were around 0.25 m/s, whereas mean values were around 0.036 m/s for the same grid. It should be noted that the convective stability condition (CFL) was always considerably less than 2 that is the restriction for convective flows. Here, however, even more restrictive conditions were used in VOF calculations. The first capillary stability condition previously proposed by Brackbill is a function of fluid density and surface tension. The second one was derived for low Re flows, ignores fluid density, but takes into account viscosity. The second condition is also generally more restrictive. No matter which stability condition was used, results from simulations were always nearly the same.

As mentioned in upper lines, there was an author's intention to have a closer look at how normals, curvatures are calculated within Fluent code and whether any more accurate procedures could be implemented instead. The 2D circle (diameter of 2 mm filled with water) patched in rectangle (4x4 mm filled with air) was used as the topology for testing of different procedures of normal and curvature calculation. Note that exact normals were known a priori and thus, might be compared with those obtained numerically. As most of commercial CFD packages also Fluent calculates normal from gradient of volume fraction, which is the easiest way, but not as accurate as will be shown later. First, normals were calculated using standard macros available in Fluent namely C_VOF_G(c,t) and C_VOF_RG(c,t). Since the surface tension model comes from work by Brackbill, also the original procedure based on ALE-like scheme was implemented via UDFs and used for calculation of normals. The worst results were obtained with the gradient macro C_VOF_G(c,t). The reconstructed macro and the procedure based on ALE-like scheme gave quantitatively very similar results. The mean deviation from the actual normal was about 0.95° and the maximum deviation was approximately 2.5°. Contrary to these, say, standard procedures, the Height Functions were employed through UDFs and the maximum deviation dropped by 300% and the mean deviation dropped even by 400 %. Unlike the foregoing procedures, the Height Functions can only be used for mapped meshes since it requires a construction of 7x3 (or 7x3) stencil in 2 dimensions around each cell containing a two phase interface. Further, based on calculated normals curvatures were determined for each interface cell. The ALE-like scheme gave evenly distributed errors no matter the orientation of normal. In some cells the error was even more than 100 %. On the contrary Height Functions exhibited far more precise results especially when the most normal direction was oriented vertically or horizontally (5 % error). However, when the normal direction was rather transverse to the grid orientation, then errors were unexpectedly even 40

%. For this reason, the new method was proposed that is in principle based on construction of circles from three points. These points are the end points of linear segments that introduce the interface. The procedure calculates curvature from the distance between the circle center and the appropriate position of the linear segment. Besides normals and curvatures, also a new volume source term for surface tension was proposed. It takes into account the length of interface within the cell and should be applied not in interface cells but rather in cells within equidistant distance of dx (size of cell) from the interface inside the denser phase. Note that neither the new method for curvature calculation nor the new volume source term for surface tension were tested practically; however, it is expected to be more accurate than the standard methods and converge with mesh refinement.

To sum up, the original objective of calculation of HTC distribution within the spreading droplet was abandoned because serious problem with surface tension model appeared. This surface tension issue was studied instead and both, new methods and results from simulations, hopefully brings an important insight into the matter.

So far only the part denoted as the micro-scale model has been discussed; however, not a single word was said about the macro scale model that should shed light on possible ways of simulating an entire water jet as a complicated droplet structure coupled with heat transfer. Considering a water jet impinging onto a hot surface, several heat transfer mechanisms can be distinguished. When the liquid temperature is below the temperature of the boiling point, then only convective-conductive heat transfer can take place. When the liquid temperature is however enhanced above the boiling point, then a certain portion of water mostly adjacent to hot surface can be evaporated and consequently transformed into either separate vapor bubbles or continuous vapor layer depending mainly on the temperature of the hot surface. Note that the word 'jet' in general does not say anything about the flow pattern. It even does not say whether the continuous flow emanating from a nozzle exit breaks into droplets or rather stays continuous. The thesis concerns with both types of jets. The first type of jet is produced by a solid jet nozzle, which can be simply e.g. just a pipe with a sharp edged exit. The second type is a flat-fan nozzle that produces a chisel-like flow pattern.

Simulations of the two phase flow outside of nozzles generally require complex inlet boundary conditions that must be either obtained experimentally or with the help of CFD. Inlet boundary conditions can be quite easily obtained from single phase simulations. Author affords to supplement the thesis with some results on the flow modeling inside the full-cone nozzle (Lechler 460.844) that were formerly cited in his master thesis. Next, the flow inside the flat-fan nozzle Lechler

(600.429.16.33) was simulated. Results such as velocities, volume fractions, and turbulent properties were later imposed in simulations of the entire jet as the inlet boundary conditions. Concerning the modeling of a solid jet, no separate single phase calculations of internal nozzle flow were performed because it was done simply together with the jet calculation within one single model. The main reason that it could be done this way is that the model was small enough in terms of number of finite volumes.

In the rest of oncoming lines the following topics will be discussed. Firstly, it will be the solid water jet impinging onto hot surface simulated using the VOF model. Secondly, it will be the single flat-fan nozzle as a representative of the whole nozzle array in the real continuous slab caster, more specifically above the first row of foot rolls, right underneath the mold bottom.

Numerical study of heat transfer between the solid jet and the hot surface required additional simulations that were used to tune up constants of k-epsilon turbulence model, namely the turbulent Prandtl number. Since the water jet spreading on surface is seemingly similar to the flow around the flat plate and reliable correlations for HTC exists for such a flow around a horizontally placed plate, simple 2D model was built up and suitable value of the turbulent Prandtl number was identified (1.3). It should be noted that the 2D model had to account for the transition from laminar to turbulent regime. The position of transition was however not calculated by the model, but it was rather defined by the correlation beforehand. Further, note that the value of 1.3 was optimal for the velocity range from 6 to 24 m/s that corresponded to radial velocities of the spreading jet. For smaller velocities the turbulent Prandtl number would be smaller and vice versa. First, a lower constant heat flux (398 kW/m^2) from heated surface was chosen in order to prevent the boiling regime. The nozzle of 2mm diameter supplied the water flow rate of 1.2 l/min. The HTC distribution was studied up to radial distance of 30 mm. Two models were tested. The first one did not account for the transition from laminar to turbulent regime, whereas the second one did so. Results were compared with experimental data and were in the good agreement. In the case of the first model, the maximum relative error was 45 %. In the second case, it was only 20 %. Note that this model was capable of simulating convective heat transfer but not evaporation. The evaporation, actually the film boiling, was taken into account in the next step.

Two different models for film boiling were put together with the help of UDFs. The first model considered that the first portion of water will evaporate within the cell of temperature higher than 150 °C. The most important assumption of the model was a steady behavior of the vapor layer, because it was designed for the steady state solver. Not many jobs were calculated, but all of them ran very fast. However, the

flow was unfortunately unsteady in terms of fluctuating vapor layer. Hence, for this particular geometry and flow settings it could not be used with success. For different flow conditions it is likely to work and due to its robustness and fast computations, it could be very useful in some applications.

Unlike the first rather unphysical and non-conservative model, the second model had a physical background. The evaporation was provided through mass and momentum source terms based on heat fluxes going always through one particular cell containing interface. The evaporation could also start from the hot wall where no vapor cells were adjacent to this wall. According to the direction of heat flux in each particular cell either the evaporation or the condensation could be present. This model came out from paper work of other researchers (Welch, Yuan). Results showed quite realistic behavior i.e. when the boiling was initiated, the jump in HTC and transition from continuous to oscillating profile was observed. However, the model was not compared with experiments and might require some minor modifications to be successfully used in any possible application.

In the thesis there is also a chapter that handles the problem of impinging solid jet in a completely different way. Instead of using the VOF model, the Discrete Phase Model was tested. The main idea consisted in significantly rougher boundary layer mesh and much lower computational costs consequently. It should be noted that using of finer mesh would not be anyhow beneficial anyway, since the rule for maximum volume fraction of dispersed phase was violated. Firstly only the cold flow namely velocity and pressure field were studied. Unlike the previous model, this model gave very uniform nearly rectangular profiles of axial velocities for the different distances from the nozzle exit. Moreover, although the interaction with surrounding air was considered, the momentum exchange was much lower than in the previous model. Nevertheless, core jet velocities were in a good agreement. On the contrary, it was not the case of radial velocities that varied much from those obtained in the previous model. Radial velocities in this model were descending much faster with increasing radial distance. As regards the pressure distribution within the nozzle footprint, the DPM model gave again almost rectangular distribution, while the previous VOF model gave more realistic Gauss-like distribution. Finally, several heat transfer calculations were performed. Firstly, only the convective heat transfer using the standard inert heating law was solved. The character of HTC distribution was relatively fine, but absolute values were far from to be desired (one order lower). This vast difference was attempted to be resolved by user defined inert heating law, which considered much higher HTC on the droplet surface. This approach however raised HTC only slightly and rather in higher radial distances than in jet axis. Employing vaporization and boiling laws gave similar

results to those using only the inert heating law. This was accredited to very poor convergence especially for continuity equation that was caused by partial violation of the rule for volume fraction of droplets. At the time of being this model is not useful for simulations of impinging solid jets.

Besides the solid jet, the jet emanating from the particular flat-fan nozzle (600.429.16.33) was investigated. Unlike the nozzle producing solid jet, this particular flat fan nozzle was chosen, since it is mounted within the real continuous slab caster and stands for the basic unit in the secondary cooling system comprising hundreds of these nozzles, manifolds and high-performance pumps. To be more specific, in this case flat fan nozzle is mounted in the first row of nozzle just above the first row of foot rolls underneath the mold bottom. In foregoing paragraphs several words were mentioned on the modeling of internal flow. Here, the results namely profiles of several variables were used as inlet boundary conditions. It is appropriate to give notice on the complexity of the computational domain. In vertical direction the fluid region is very narrow e.g. the flat jet passes the foot roll only in distance of several millimeters. Further, the flat jet hits the very hot slab surface (>1000 °C), its flow veers left, right, down, and up rapidly to be veered soon again by symmetry conditions, mold at the top, and the foot roll in the bottom. Moreover, the angle of zero can be found between the slab and the foot roll. This closely tighten up space must definitely cause tremendously unstable and turbulent flow that makes calculations more difficult.

It was decided to solve this using the Euler-Euler model. Since this model is not capable of predicting the secondary breakup, the breakup model based on WAVE model was developed and employed using UDFs. It was tested on 2D jet. Although it successfully predicted the evolution of parent droplet diameters, it did not account for diameters of child droplets. This could be overcome using some averaging method and thus obtain a mean diameter within each cell that would represent both, parent and child diameters. This was however considered only theoretically; therefore, only the constant droplet diameter was considered within the Euler-Euler model. Later on, using of the Euler-Euler model was not anyhow advantageous because it required very small time steps (5e-06 s). To make matters worse, the model suffered from the lack of water along the center line of flat jet which was pretty weird on the one hand but on the other hand it was confirmed by literature (St-Georges and Buchlin).

Because of these bottlenecks, the Discrete Phase Model was used instead. Inlet boundary conditions were determined from internal flow simulations. The primary breakup was simulated using the flat fan atomization model. As regards the

secondary breakup, both, the Taylor Analogy (TAB) and the Blob jet breakup models, were tested. Experimental data (velocity and droplet distributions) were used to tune up the model constants. The TAB model gave markedly more accurate results than the Blob jet model. For the number of parcels of 2000 and streams count of 10 results agreed very well with experimental data. Since the discrete phase cannot be formed into a continuous fluid region and this is actually what seemingly happens in the gap between the slab and the foot roll, the model for coupling between the discrete phase and the continuous phase was developed and tuned in terms of mass conservation. To make a picture complete, the discrete phase was simulated by the DPM model, whereas the continuous phase was simulated by the VOF model. Because of a certain smearing of free interface the drag force acting on each droplet had to be modified i.e. up to a specific water volume fraction limit the droplet behaved like it was passing only through a cell containing 100 % of air. Similar but much more complicated changes would have to be done to secondary breakup model, but in this case the secondary breakup was simply rather not taken into account. The model for coupling was quite robust, but most importantly, results were likely to be realistic.

In next step, the heat transfer was included but the temperature of mold was lowered from more than 1000 °C to 200 °C to avoid large source terms. For these ‘kick-off’ simulations the model for coupling was not considered. Several model settings were tested and especially strong dependence on boundary layer was identified. The thinner the first cell layer was, the worse convergence behavior was detected. Of course, this was caused by violating the rule for the maximum allowed volume fraction of dispersed phase within each particular cell. On the other hand, the thinner the layer was, the more accurate results were gained. Results were ranging from 10 kW/m^2 for rough mesh to 100 kW/m^2 for fine mesh. The reality can be still even one order higher. This incapability of the present model can be explained simply explained by the very low heat transfer between the hot slab and the droplet. The first responsible originator could be the missing radiation exchange between the slab and the semitransparent droplet. The second originator definitely is the low temperature in cell adjacent to hot slab that is consequently used for calculation for the calculation of evaporative heat transfer. It might be useful to hold temperature of near slab cells at temperature of the slab and perhaps it might be also useful and more realistic to keep the vapor fraction equal to unity. These proposals were however not put in practice.

To summarize the thesis it is convenient to define three different 'folders' in which each particular piece of this thesis can be filed separately. Let's start with the folder

that does not sound just good. In here, we could leave numerical models that led into blind passage such as the simulation of 0.2mm droplet free-falling and finally impinging on hot surface using the standard surface tension model or the Euler-Euler model in modeling of flat jet as a basic unit in continuous slab caster etc. The second folder sounds somewhat better, because in there we can place models and ideas that were partially able to solve the problem, but would require other subroutines or modifications that would lead to desired results. Frankly, it could not be brought to an end, since it would be too much extensive work that would definitely ask for more time to spend on it. In this second folder we could put e.g. the secondary breakup model for the Euler-Euler model or the new approach for implementation of Capillary forces. At last, the third folder can be filled in with models, simulations that worked reliably e.g. subroutines for calculation of interface normals and curvatures within the VOF model, numerical study of HTC distribution for solid jet spreading on hot surface with the temperature below the boiling point, simulation of flat jet using the DPM model, the model for coupling between the DPM and the VOF model.

The author is pretty sure that there might be some mistyped characters, discrepancies, imperfections, but in the same measure he is convinced that the thesis can yield notable profit to other researches.

5 SELECTED BIBLIOGRAPHY

[1] FRANCOIS, M., *Computations of drop dynamics with heat transfer*, Doctoral thesis, University of Florida, 2002

[2] WELCH, S.W.J., WILSON, J., *A Volume of Fluid Based Method for Fluid Flows with Phase Change*, Journal of Computational Physics, vol. 160, pp. 662-682, 2000

[3] YUAN, M.H., YANG, Y.H., LI, T.S., HU, Z.H., *Numerical simulation of film boiling on a sphere with a volume of fluid tracking method*, International Journal of Heat and Mass Transfer, vol. 51, pp. 1646-1657, 2008

[4] LUNKAD, S.F., BUWA, V.V., NIGAM, K.D.P., *Numerical simulations of drop impact and spreading on horizontal and inclined surfaces*, Chemical Engineering Science, vol. 62, pp. 7214-7224, 2007

[5] ADLER, W.F., *Waterdrop impact modeling*, Wear, vol. 186, pp. 341-351, 1995

[6] CHO, M.J., THOMAS, B.G., LEE, P.L., *Three-Dimensional Numerical Study of Impinging Water Jets In Runout Table Cooling Processes*, Metallurgical and Materials Transactions B, vol. 39, pp. 593-603, 2008

[7] KULJU, T., MAURINEN, E., KEISKI, R., *Filmboiling studies with CFD*, Proceedings of the EnePro conference, pp. 117-119, 2009

[8] NARUMENCHI, S., TROSHKO, A., BHARATHAN, D., HASSANI, V., *Numerical simulations of nucleate boiling in impinging jets: Applications in power electronics cooling*, International Journal of Heat and Mass Transfer, vol. 51, pp. 1-12, 2008

[9] BHATTACHARYA, P., SAMANTA, A.N., CHAKRABORTY, S., *Spray evaporative cooling to achieve ultra fast cooling in runout table*, International Journal of Thermal Sciences, vol. 48, pp. 1741-1747, 2009

[10] G. STROTOS, M. GAVAISES, A. THEODORAKAKOS, G. BERGELES, *Numerical investigation of the cooling effectiveness of a droplet impinging on a heated surface*, Heat Mass Transfer, 2008, doi:10.1016/j.ijheatmasstransfer.2008.02.036

[11] BRACKBILL, J.U., KOTHE, D.B., ZEMACH, C., *A continuum method for modeling surface tension*, J. Comput. Phys. 100 (1992) 335–354

[12] GALUSINSKI, C., VIGNEAUX, P., *On stability condition for bifluid flows with surface tension: Application to microfluidic*, Journal of Computational Physics volume 227, pp. 6140-6164, 2008

[13] UBBINK, O., ISSA, R.I., Method for Capturing Sharp Fluid Interfaces on Arbitrary Meshes, J. Comput. Phys., 153, 26-50, (1999)

[14] AFKAMI, S., BUSSMANN, M., *Height Function-Based contact angles for VOF simulations of contact line phenomena*, International Journal of Numerical Analysis and Modeling, Volume 1, pp. 1-18, 2004

[15] AFKHAMI, S., BUSSMANN, M., *Height functions for applying contact angle to 2D VOF simulations*, International Journal for Numericla Methods in Fluids, Volume 57, pp. 453-472, 2008

[16] RUDMAN, M., A Volume-tracking Method for Incompressible multifluid flows with large density variations, Int. Journal for Numerical methods in Fluids , Volume 28, pp 357-378, 1998

[17] CUMMINS, S. J., FRANCOIS, M. M., KOTHE, D. B., *Estimating curvature from volume fractions*, Computers and Structures, Volume 83, pp. 425-434, 2005

[18] SCHILLER, L., NAUMANN, Z., Z.Ver.Deutsch. Ing., pp.77-318, 1935

[19] RANZ, W.,E., MARSHALL, JR., *Evaporation from drops, part I.*, Chem. Eng. Prog. Vol. 48, pp. 141-146, 1952

[20] RANZ, W.,E., MARSHALL, JR., *Evaporation from drops, part II.*, Chem. Eng. Prog. Vol. 48, pp. 173-180, 1952
[21] LUXFORD, G., Experimental and modelling investigation of the deformation, drag and break-up of drizzle droplets subjected to strong aerodynamic forces in relation to SLD aircraft icing, PhD thesis, Cranfield university, 2005
[22] INCROPERA, F. P., DE WITT, D. P., *Fundamentals of Mass and Heat Transfer*, John Wiley & Son, Third edition, pp. 393-395, 1990
[23] http://www.fluentusers.com/fluent/doc
[24] WU, S., SHIN, C. H., KIM, K. M., CHO, H. H., Single-phase convection and boiling heat transfer: Confined single and array-circular impinging jets
[25] HALL, D.E., INCROPERA, F. P., VISKANTA, R., Jet Impingement Boiling from a circular free-Surface Jet During Quenching: Part 1 – Single-Phase Jet, Journal of Heat Transfer, vol. 123, pp. 901-910, 2001

6 AUTHOR'S CURRICULUM VITAE

Personal information:

Name:	Jan Boháček
Address:	Mladkov 95, Skalice nad Svitavou, 679 01
Phone:	+420728223236
Place of birth:	Boskovice
Date of birth:	23. 4. 1982
Marital status:	single

Education:

2001–2006	Brno University of Technology, Faculty of Mechanical Engineering, Kaplan Department of Hydraulic Machines, Thesis: Ejector type cooling nozzle
1997–2001	Gymnázium Boskovice, Palackého nám. 1

Experience:

2008	Internship: Continuous casting problems solved in Fluent, CFD group in CORUS, Netherlands Supervisor: Dr. Tim Peeters
2010	Cooperative researcher: Heat transfer simulations and measurement at Heat Transfer and Fluid Flow Laboratory, Brno University of Technology
2011	Scientific staff: Chair of Simulation and Modelling of Metallurgical Processes, Montan University of Leoben

Languages and other skills:

Languages	English (fluent), German (basics)
CFD	Fluent, Gambit, ICEM
Programming	MATLAB, C for Fluent
Graphics:	AutoCAD, SolidWorks

7 ABSTRACT

The present thesis is focused on an overall description of water jets and air atomized jets for cooling purposes using CFD methods namely ANSYS FLUENT. It comprises two main parts – the micro and the macro model. The micro model concerns with a numerical description of single droplet dynamics whereas the macro model deals with a numerical modeling of water jets as complicated droplet structures emanating from solid stream nozzle and flat fan nozzle. By and large, it is based on multiphase models and User Defined Functions (UDFs), which represents the background of the present thesis. In most of cases, the presented numerical models were compared either with experimental data or another numerical model.

In the first part, the theory of each of three multiphase models is discussed. The first one, the Volume Of Fluid model (VOF), was used for simulation of single droplet dynamics designated as a micro model whilst last two multiphase models, the Euler-Euler model and the Euler-Lagrange model, were applied in the case of modeling of the entire water jet structure, which is contrarily designated as a macro model.

The micro model concerns with a numerical study of free-falling water droplet. For small droplet diameters (~100μm) the standard surface tension model (Continuum Surface Force model, CSF) was proved to cause significant unphysical parasitic currents. Therefore, the thesis is also devoted to surface tension as a source term of body forces imposed in momentum equation, normal, curvature calculation and related issues.

The macro model covers a numerical study of dynamics of the entire water jet structure i.e. the space between the nozzle exit and the wall where the jet impinges. It accounts for the complete geometry, for instance, support rolls, a slab and a mold bottom of a continuous caster.

Firstly, the physics of a solid jet impact onto a hot plate was simulated using both, the VOF and the Euler-Lagrange model. As regards the case with the VOF model, a model for film boiling was designed and tested.

Finally, both, the Euler-Euler model and the Euler-Lagrange model, were used for simulation of a flat jet horizontally spraying onto a hot slab inside a confined domain bounded by support rolls and a mold bottom. Concerning the simulation with the Euler-Euler model, a secondary breakup model was introduced based on the wave stability atomization theory. Concerning the Euler-Lagrange simulation, the dispersed phase (Lagrange particles) formed rather a continuous phase in some places, and therefore the coupling between Lagrange particles and the VOF model via UDFs was proposed.

8 ABSTRAKT (ČESKÝ)

Práce komplexně popisuje vodní a vodovzdušné chlazení pomocí metod CFD (Computational Fluid Dynamics) konkrétně s využitím softwaru ANSYS FLUENT. Skládá se ze dvou hlavních částí, z nichž první se zabývá numerickým popisem jediné vodní kapky a druhá popisem směsí kapek představující paprsek válcové a ploché trysky. Je založena převážně na vícefázových modelech proudění a vlastních uživatelsky definovaných funkcí (User Defined Functions, UDF) představujících stěžejní část práce. Uvedené výpočtové modely jsou ve většině případů verifikovány pomocí experimentálních dat nebo jiných numerických modelů.

V první části práce jsou teoreticky postupně rozebrány všechny tři použité vícefázové modely proudění. První z nich, Volume Of Fluid model (VOF), byl použit pro modelování jediné kapky (mikromodel). Zatímco zbývající dva, Euler-Euler model a Euler-Lagrange model, byly aplikovány v modelu celého paprsku trysky (makromodel).

Mikromodel popisuje dynamiku volného pádu vodní kapky. Pro malé průměry kapek (~100 μm) standardní model povrchového napětí (Continuum Surface Force, CSF) způsoboval tzv. parazitní proudy. Z toho důvodu je v práci rozebrána problematika výpočtu normál, křivostí volných povrchů a povrchového napětí jako zdroje objemových sil v pohybových rovnicích.

Makromodel se zabývá studiem dynamiky celého paprsku tj. oblastí od ústí trysky po dopad na horký povrch, bere v úvahu kompletní geometrii, tzn. např. podpůrné válečky, bramu, spodní část krystalizátoru apod.

V práci je rozebrána 2D simulace dopadu paprsku válcové trysky pomocí VOF modelu Euler–Lagrange modelu na horký povrch. Pro případ s VOF modelem byl navržen model blánového varu.

Euler–Euler model a Euler–Lagrange model byly využity pro simulaci paprsku ploché trysky horizontálně ostřikující horkou bramu přímo pod krystalizátorem nad první řadou podpůrných válečků. Pro Euler-Euler model byl navržen model sekundárního rozpadu paprsku založený na teorii nejstabilnější vlnové délky (Blob jet model). Jelikož diskrétní Lagrangeovy částice tvořily v určitých místech spíše kontinuální fázi, byl navržen a otestován model pro konverzi těchto částic do VOF modelu.